



CHANCE project

(Contract Number: 755371)

Report on tuned algorithms and their performance

DELIVERABLE (D4.3) Work Package 4

Author(s): A.F. Alrheli, D. Barker, C. De Sio, D. Kikola, A.K. Kopp, M. Mhaidra, J.P. Stowell, L.F. Thompson, J.J. Velthuis, M.J. Weekes

Reporting period 3: 01/06/2020 – 31/03/2022

Date of issue of this report: April 2022

Start date of project: 01/06/2017

Duration: 58 Months

This project has received funding from the Euratom research and training programme 2014-2018 under grant agreement No 755371;

Dissemination Level		
PU	Public	X
CO	Confidential, only for partners of the CHANCE project and EC	

History chart			
Status	Type of revision	Partner	Date
Draft	Initial version	USFD/ UNIVB R I S / WUT	

Reviewed by

Approved by

The Executive Board

Section 1: Introduction

The CHANCE project [1] aims to address the specific issue of the characterisation of conditioned radioactive waste. The characterisation of fully or partly conditioned radioactive waste is a specific issue because unlike for raw waste, its characterisation is more complex and therefore requires more advanced non-destructive techniques and methodologies.

The objective of CHANCE is to further develop, test and validate techniques already identified that will improve the characterisation of conditioned radioactive waste, namely those that cannot easily be dealt with using conventional methods. Specifically, the work on conditioned radioactive waste characterisation technology will focus on:

- Calorimetry as an innovative non-destructive technique to reduce uncertainties on the inventory of radionuclides;
- Muon Tomography to address the specific issue of non-destructive control of the content of large volume nuclear waste;
- Cavity Ring-Down Spectroscopy (CRDS) as an innovative technique to characterise outgassing of radioactive waste.

The present report focuses on activities from Work Package 4 related the development of Muon System and discusses simulations-based studies of algorithm performance, object size and position reconstruction of a system analogous to that built at Bristol.

An exhaustive series of simulations were performed to assess the expected size and position resolution of any expected feature in a waste drum as a function of the system parameters for a system analogous to that used in WP4. In order to place a quantitative, rather than qualitative measure on our result, an approach to this study, similar to those practised in the (analogue) photographic industry, using so-called “figures of merit” was adopted. This work, presented in Section 2 below, addresses a number of open questions such as the expected resolution of the size of any reconstructed feature along with the relationship of feature resolution with exposure time. These studies have been presented in a number of forums including international conferences and received particular interest at the WM2019 conference.

The study of features of high density in a CASTOR or similar waste drum is important for locating high-Z materials with muon scattering tomography. However, of equal importance is the ability to identify areas of under-density since they may indicate features such as differential settlement in the matrix or, more importantly, the presence of gas bubbles in the matrix due to outgassing effects. Such bubbles are a concern since they may lead to pockets of high-pressure gas in the waste drum which could be of concern to the structure of the waste drum. Section 3 describes the ability of the muon scattering tomography technique to locate and qualitatively measure such voids. This work performs a study of the response of MST algorithms to the presence of a void in the drum matrix. Tests are also, successfully, performed in the presence of other materials. Importantly the muon tomography method is not only capable of identifying the location of the bubble but also shows a remarkable ability in reconstructing the bubble volume with excellent linearity in the relationship between the reconstructed and actual bubble size.



Finally, Section 4 reports on a further study which has taken a number of the key, tuned algorithms that are used globally in Muon Scattering Tomography (MST) community and ground-breaking work has been performed in qualitatively comparing the performance of different standard algorithms that are used in MST. By choosing a suitable figure of merit metric (i.e. the ‘Contrast to Noise ratio’) quantitative comparisons have been made, allowing, for the first time, the worldwide muon tomography community to assess the relative merits and performance metrics for these different algorithms. This work on algorithm comparisons has been presented in conferences and, in addition, has recent been written up as a scientific journal article that has been submitted to IOP Publishing’s Journal of Instrumentation (JINST).

Section 2: In-drum feature and size figures of merit [5]

Figure of merit tests were developed to enable the imaging performance of standard muon tomography algorithms to be compared to one another. A feature resolution test was developed to understand an algorithm’s ability to separate and distinguish high density objects in close proximity to one another. A size resolution test was also developed to understand the smallest object that can be observed by a given tomography algorithm.

In each case 3 different algorithms were considered, namely: 1/ the simple Point-of-Closest Approach [2], 2/ the Angle Statistics Reconstruction [3], and 3/ the Binned Clustering Algorithm [4]. Each of these algorithms divide the volume of interest up into a 3D grid of cubic voxels with a side length of 1cm. A discriminator score is then derived from all muon trajectories that pass through a given voxel so that regions of high and low density can be mapped inside a waste drum.

The Point-of-Closest Approach (PoCA) algorithm simply assumes that any muon must have undergone a single scattering inside the volume of interest. Since large scattering angles indicate the presence of high density materials, each voxel is weighted by the median angle of all muon trajectories whose point of closest approach is inside the given voxel. This is one of the simplest muon tomography algorithms available but benefits from being the least computationally intensive.

The Binned Clustering (BC) algorithm assumes that in low density material, scattering vertices inside a single voxel will be more distributed than in high density materials such as uranium. A high momentum muon is also more likely to undergo large scatters only when passing through a dense material. A discriminator is calculated based on these two assumptions by calculating the metric distance between pairwise combinations of different muon points of closest approach, r , inside a voxel:

$$m_{ij} = \frac{\|\vec{r}_i - \vec{r}_j\|}{\theta_i p_i \theta_j p_j} \quad (1)$$

Where \vec{r}_i is the point-of-closest approach for muon i , and θ_i and p_i are the muon scattering angle and momentum respectively. The median of all calculated metric distances in each voxel can be used to discriminate different materials.



In reality, as a muon traverses a waste drum, it is more likely to undergo a number of small scatters instead of a single large, localised scatter as assumed in the PoCA algorithm. The PoCA algorithm is therefore prone to additional noise if a muon trajectory is mis-reconstructed so that it appears as an extreme scattering vertex inside a single voxel. The Angle Statistics Reconstruction (ASR) algorithm tries to account for this by considering all voxels that lie within a chosen minimum range of the muon trajectories reconstructed before and after the volume of interest. This removes the assumption that a muon scatters inside only a single voxel, leading to reduced noise in the output density map.

A large number of Monte Carlo simulations were performed to compare different aspects of detector performance, such as feature and size resolution and the dependence on exposure time and material type. All of this was performed quantitatively, rather than qualitatively, by the introduction of a suitable figure of merit. In all cases the assumed detector system for the studies was the CHANCE muon tracking system comprising drift chambers with 2 mm position resolution and RPCs with 0.3 mm resolution. In this case the results of the simulations are directly relevant to the CHANCE muon system.

Two figure of merit tests were developed so that the imaging performance of the 3 algorithms can be compared to one another. A feature resolution test was developed to understand an algorithm's ability to separate distinguish high density objects in close proximity to one another. Similarly, a size resolution test was developed to understand the smallest object that can be observed by a given tomography algorithm.

To understand feature resolution, an array of 20 cuboid uranium target objects was simulated, each with sides of 10 cm in the Y and Z dimension embedded in a concrete-filled nuclear waste drum of dimensions 88 cm high and 57 cm in diameter. Starting with a X dimension thickness of 10 cm, the thickness and spacings in the X dimension were reduced by a factor of 75% for each successive target object as shown in Figure 1. Scanning from left to right, the number of observable features gives a metric for the smallest observable feature and separation combination achievable when the given analysis technique was applied to the muon trajectories reconstructed in the detector under consideration. If N_0 is the number of objects clearly observable, the minimum feature size is:

$$x_{min} = 10 \text{ cm} \times 0.75^{N_0-1} \quad (2)$$

Detectable size resolution was considered in a similar way by taking an array of 8 cuboid uranium target simulated objects, each with sides of 10 cm in Y and Z. Starting at a X dimension of 3 cm, the thickness in the X dimension was then scaled by a factor of 75% for each successive target object, as shown in Figure 2, whilst the object spacing was kept fixed. Scanning from left to right, the number of observable features gives a metric for the smallest observable feature when objects are not in close proximity to one another. If N_0 is the number of objects clearly observable, the smallest observable object is given by:

$$s_{min} = 3 \text{ cm} \times 0.75^{N_0-1} \quad (3)$$



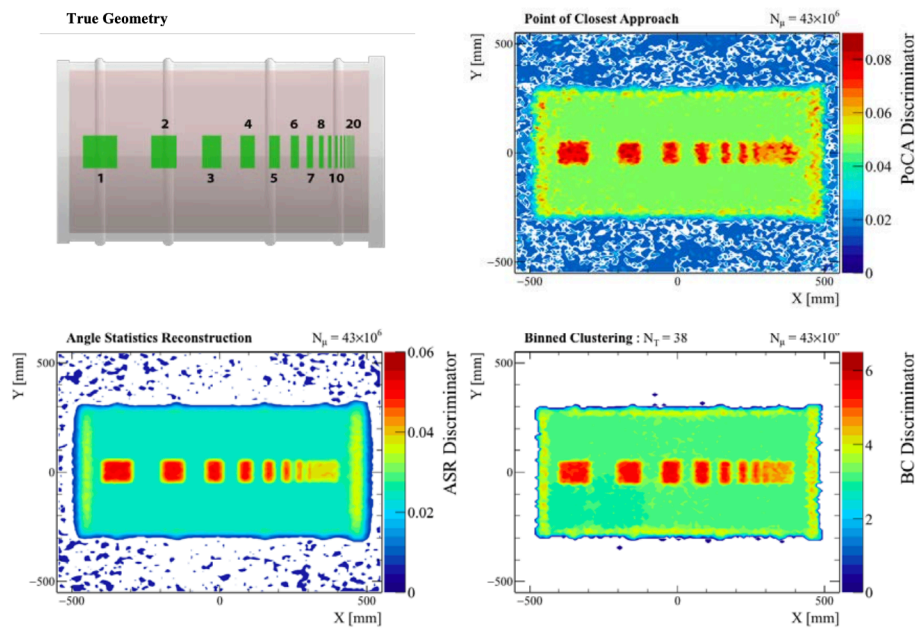


Figure 1: Uranium feature resolution test images after 25 days of simulated cosmic ray exposure. The number of observable objects gives an indicator on the resolution of each imaging technique. It is only possible to observe 6 separated objects using the PoCA algorithm, whilst the ASR and BC algorithms can both make out an additional feature.

Figure 1 clearly shows, for example, that the PoCA algorithm is only capable of clearly resolving 5 objects, corresponding to a smallest observable object of 0.95 cm, comparable to the voxel size. In contrast, the ASR and BC algorithms both show much cleaner, rectangular features for all 8 objects, resolving the presence of a target object down to 4mm. This information helps to educate what algorithms we would use to analyse data from the CHANCE muon tracking system.

Finally, the importance of establishing a “figure of merit” is exemplified in Figure 2 which took one of the better-performing algorithms, namely binned clustering (BC) and considered the output density maps for the feature and size resolution tests after shorter cosmic ray exposures. After just 4 days of exposure, noise in the density maps means only 5 objects were clearly distinguishable, whilst little difference was found between 16 and 25 days of exposure. This highlights the fact that eventually a statistical limit is reached in which the output image is constrained only by the angular resolution of the detector itself.

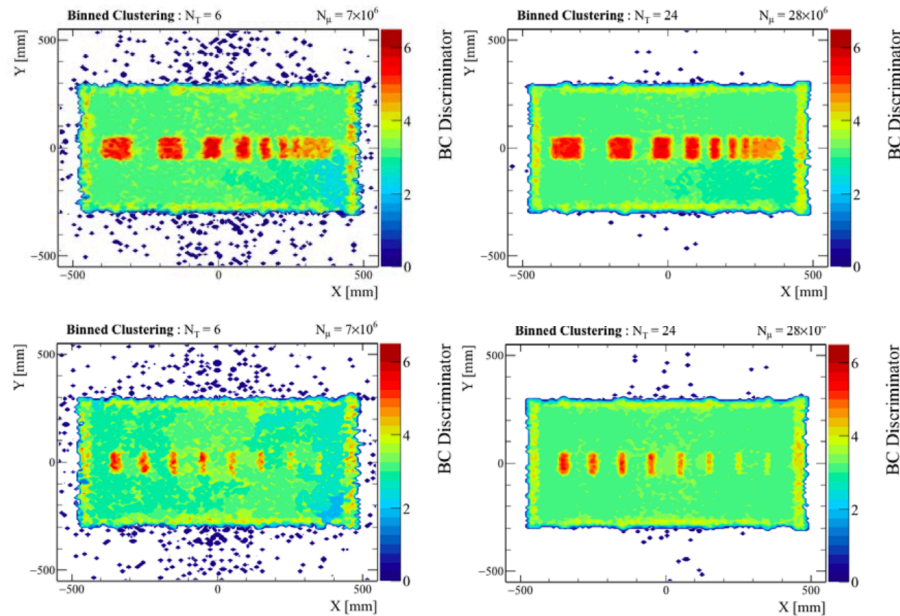


Figure 2. Uranium feature (top) and size (bottom) resolution test images after 4 days (left) and 16 days (right) of simulated cosmic ray exposure. The feature and size resolution improves with longer exposure times, eventually reaching a limit where the detector angular resolution defines the minimum observable feature.

Section 3: Identification and measurement of gas bubbles in bitumen waste drums [8]

Whilst the identification and classification of areas of over density (i.e. high Z materials) is of primary importance and interest when applying muon scattering tomography to the imaging of nuclear waste drums, there is also a need to be able to identify lower density regions, and in particular voids, in any drum as they may indicate the dangerous build-up of gases.

Self-irradiation of bituminous packages containing radioactive waste generates gases arising from the radiolysis of the bitumen, of which hydrogen is the most abundant. If the rate of gas production exceeds the capacity of gas release by diffusion, hydrogen bubbles are created and bituminous matrix can occur. The ability to detect the amount of gas formed in the waste containers and to determine whether the gas formed is evenly distributed in small bubbles or concentrated in bigger bubbles is therefore of paramount importance from a repository safety perspective.

Simulations were performed with the Geant4 [6] particle physics software which is a toolkit for simulating the passage of particles through matter. The cosmic ray generator CRY [7] was used to create muons with the appropriate angle and momentum distributions. The volume simulated was a cylinder of a concrete-like material with a density of 2.3 g/cm³, encased in a steel container. The simulated detectors were assumed to be the University of Bristol resistive plate chambers (RPCs) previously developed at the University of Bristol each with an active area of 1x1 m² and an assumed position resolution of 450 μm. Each simulation

comprised 159 million muons, corresponding, for this detector size, to about 16 days of data taking.

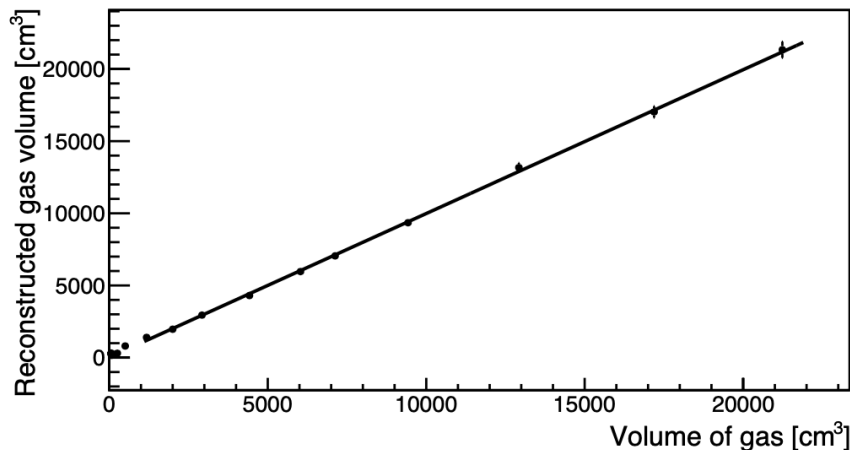


Figure 3: Reconstructed volume of the bubbles as a function of the simulated volume.

A method to identify low-Z and low density materials embedded in a higher Z concrete-like material was developed which works as follows. The volume of interest is divided into cubic bins of 1 cm³. A fixed number of the most scattered tracks reconstructed in each bin is selected, and for each pair of tracks a metric distance m_{ij} is calculated following the expression given in equation 1 above. The distributions of $\log(m_{ij})$ are obtained for all the bins and their medians were chosen as a discriminator value. By plotting the discriminator value for the bins from a drum filled only with gas and another with only concrete it was found that the mean of this discriminator distribution function, μ_{disc} , is the variable that depends the most on the gas volume and hence gives the greatest discrimination power between an volume in a drum that is a gas bubble and a volume that consists of the concrete matrix.

The mean of the discriminator was calculated for each bubble size and compared to the real volume simulated (V), resulting in a linear relation for volumes of 2 litres or more. A straight line was fitted to the graph of μ_{disc} as a function of the volume V (for bubbles of 1 litre or more). This straight line fit equation was then used to calculate calibrated volumes, which are shown in Fig. 3 as a function of the simulated gas volumes. There is a remarkable linearity in the relationship between the discrimination variable and the real gas volume, right down to small gas volumes. The relative uncertainty of the reconstruction of gas volumes of 2 litres or more was low, with a resolution of $1.6 \pm 0.8\%$. The relative uncertainty obtained for a 1 litre bubble was 19%.

Section 4: A quantitative assessment of the imaging of high and medium Z materials using muon scattering tomography [9]

In this final section we report on the results of an exhaustive set of detailed simulations that have been performed to assess the performance of the CHANCE instrumentation when using a number of different muon scattering tomography algorithms applied, specifically, to the imaging of nuclear materials that have been stored in either a small nuclear waste drum or a CASTOR V/52 type nuclear waste drum. The following is a brief synthesis of a 24-page journal submission to the JINST journal.

As in the studies presented above, the three most popular (in the muon scattering tomography community) reconstruction techniques of Point of Closet Approach (POCA), Binned Clustering (BC) and Angle Statistics Reconstruction (ASR) were considered. Once again, the detection system considered for the studies was that developed by Bristol and Sheffield for CHANCE WP4. One important feature introduced in this study however is the so-called contrast to noise ratio (CNR value), a metric that permits the quantitative comparison of the performance of different algorithms when imaging target materials defined as:

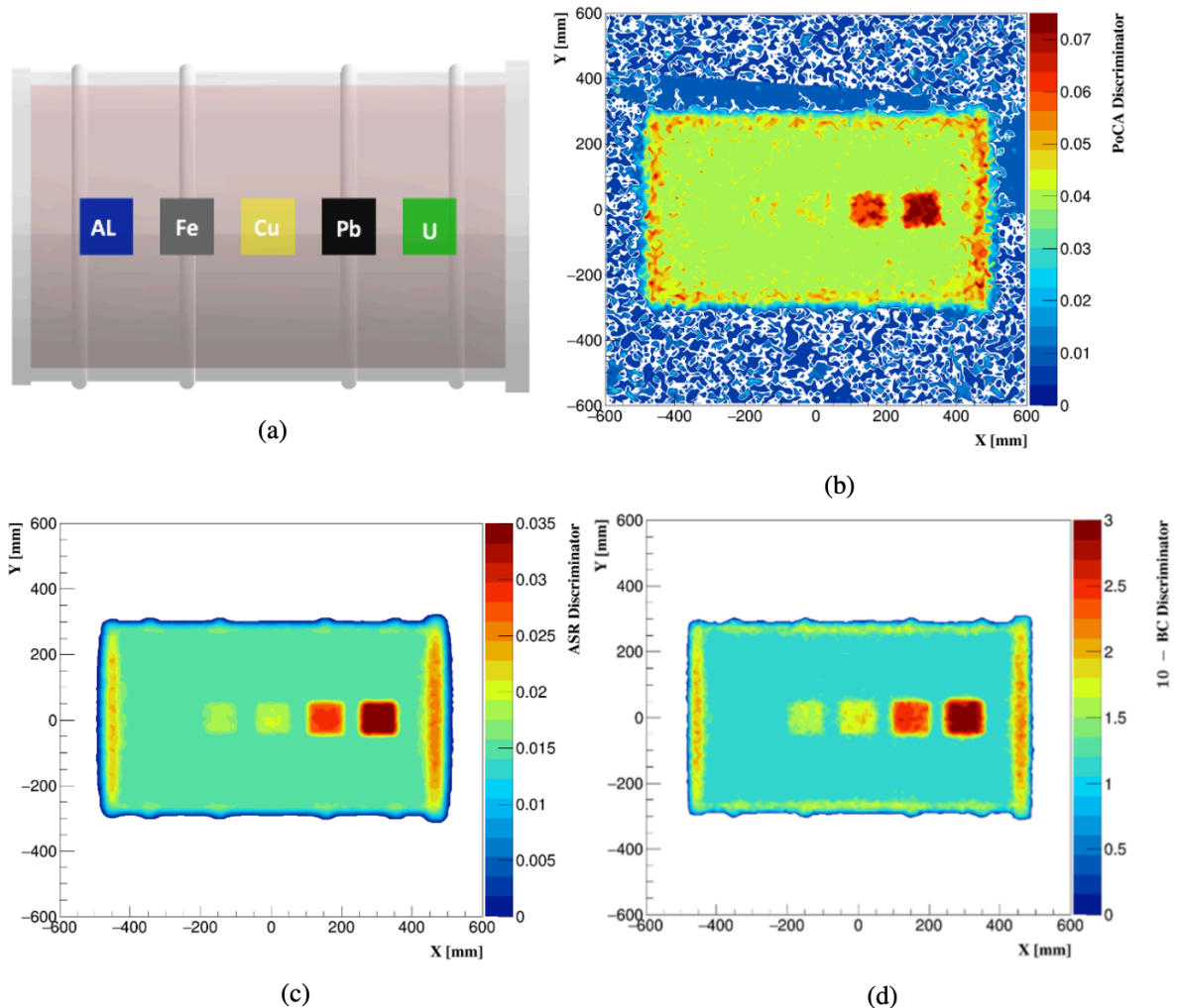
$$\text{CNR} = \frac{|\mu_A - \mu_B|}{\sqrt{\sigma_A^2 + \sigma_B^2}} \quad (4)$$

where μ_A is the mean of region A's signal and μ_B is the mean of region B's signal. σ_A and σ_B are the standard deviations of the signals in region A and region B, respectively.

This study was performed for 2 different formats of nuclear waste drum size. In the first instance this was a small nuclear waste drum which is made of steel (~92% iron and 2% carbon) and is of 96 cm length and 57.4 cm diameter. It is filled with concrete to a total diameter of 52.4 cm and has a density of 2.3 g/cm³. These characteristics were chosen to be similar in format to the drum to be imaged in the CHANCE detector system. The three reconstruction algorithms discussed above were each used to image five target materials that varied in density from 2.699 g/cm³ (aluminium) to 18.59 g/cm³ (uranium) - see figure 4(a). The dependence of the results on the size and location of the target materials as well as the muon exposure time was considered.

First the performance of the 3 reconstruction techniques using a fixed muon exposure time was considered. The performance of each method is represented quantitatively by the CNR value between two different regions after 30 days of muon exposure time. The sliced outputs shown in Figure 4 are taken through the 3D density maps along the centre of the drum. In this case the target materials are of size 10 x 10 x 10 cm³ inside the waste drum. The outputs clearly show that all three reconstruction methods are able to locate high-Z materials (U and





Pb) shielded by the concrete matrix, whereas the POCA method failed to identify the medium-Z target materials (Cu and Fe) - see Figure 4(b).

Figure 4: (a) Target materials inside the simulated drum. X-Y slice outputs through the 3D density map from applying the (b) POCA, (c) ASR, and (d) BC algorithms respectively. The exposure time was fixed at 30 days equivalent. The BC algorithm considered the 38 most scattered tracks per voxel (N).

For the low-Z target material, all methods are unable to separate the aluminium cube from the background, this is to be expected since the muon scattering technique is primarily sensitive to density and aluminium has an almost similar density to the concrete. Figure 5 shows the CNR results of all algorithms used after 30 days of muon exposure when comparing the five target materials, namely uranium, lead, copper, iron, and aluminium with the regions that are constructed of “background signals”, i.e. the waste drum matrix - in this case concrete. The BC and ASR algorithms demonstrate very similar performance when comparing the regions that contain a cube of high-Z material (uranium) against the background regions. In the case of a 10 cm cube the BC method produces a slightly lower

CNR value of 7.1 ± 0.34 compared to the CNR value of 7.9 ± 0.25 produced by the ASR algorithm.

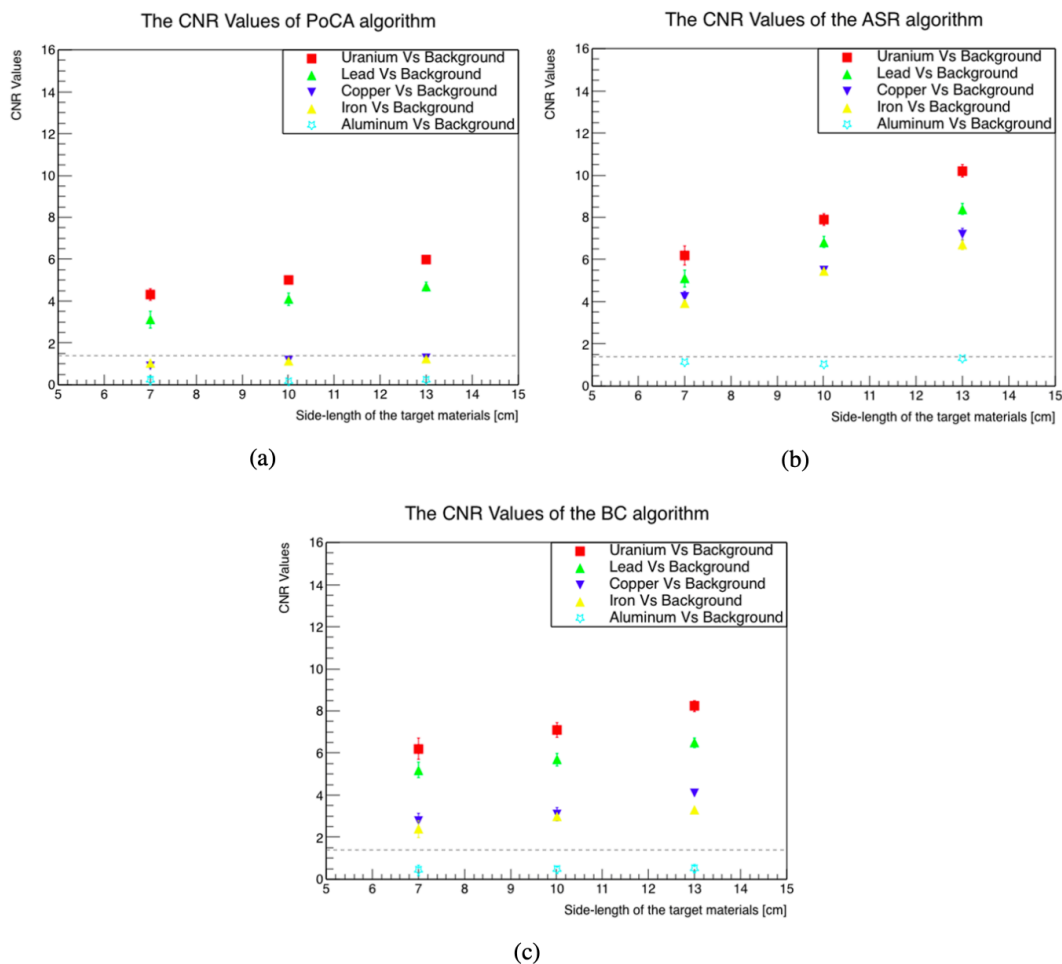


Figure 5: Comparison of the CNR values of the (a) PoCA, (b) ASR and (c) BC algorithms when differentiating between different target materials and background for target materials with side lengths of 7, 10, and 13 cm. Results are for 30 days of muon exposure time. The horizontal dashed line represents the minimum CNR value used to distinguish the target material inside the drum.

The PoCA method is limited by the single-scattering assumption, which leads to adding more noise which reduces the CNR values between the compared regions inside the drum. For example, for 10 cm sided cubes the PoCA algorithm has only been able to distinguish the uranium and lead from the background with relatively low CNR values of 5.0 ± 0.2 and 4.1 ± 0.3 , respectively. The results from comparing the regions containing copper and uranium reveal that the ASR algorithm is the most capable of differentiating between medium-Z and high-Z materials with a CNR value of 5.35 ± 0.1 , which is approximately 34% better than the CNR value produced for the comparable regions by the BC method. In terms of the size dependence, the CNR results from comparing the target regions showed that the ASR is more likely to be impacted by the target region's size. For example, comparing lead cubes



against background regions showed almost a 65% increase in the CNR values from 5.1 ± 0.4 to 8.4 ± 0.26 when the side-length of the lead cube increased from 7 cm to 13 cm.

These studies were subsequently repeated to understand the affect of muon exposure time on the overall ability to image and differentiate different materials within a concrete matrix. The corresponding CNR plots for the different muon scattering tomography reconstruction algorithms are depicted below in figure 6. Clearly, as expected, the CNR value, and hence ability to differentiate between different materials, increases with the exposure time. Of note here however is that the PoCA algorithm performs worst of the 3 algorithms considered, for the single point of scattering reason as discussed earlier. For low exposure times the ASR algorithm clearly outperforms its competitors, however its performance as a function of exposure time (as measured by the CNR metric) tends to plateau rapidly whilst the BC algorithm showed a marked improvement with exposure time. In general, for all cases considered here the ASR algorithm shows the best performance.

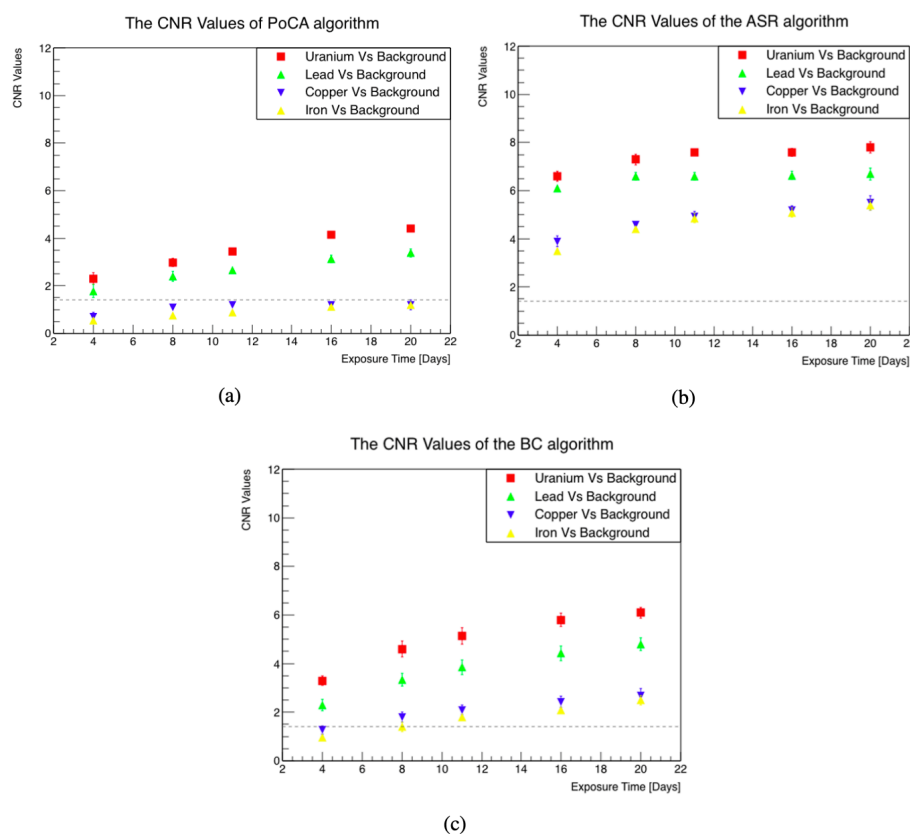


Figure 6: Comparison of the CNR values produced by the (a) PoCA, (b) ASR and (c) BC algorithms for different materials of 10 cm side-length as a function of the muon exposure time. The horizontal dashed line represents the minimum CNR value used to distinguish the target material inside the drum.

As a final investigation this systematic study considered a life-size CASTOR V/52 drum and looked at whether or not muon scattering tomography could identify any material diversion that had taken place in the drum. Such diversion scenarios are an important consideration



when considering the long-term safety and safeguarding of nuclear waste and muon tomography offers a unique, non-invasive and non-destructive, means to perform such checks.

In this study a CASTOR V/52 was assumed to have been illegally interfered with in such a way as a number of diversions of nuclear materials have taken place. Specifically, the following diversion scenarios were considered (numbers refer to figure 7(a)): 1/ half-loaded basket (side), 2/ half-loaded basket (centre) 3/ fully-unloaded basket 4/ basket where UO₂ pellets have been replaced with Copper.

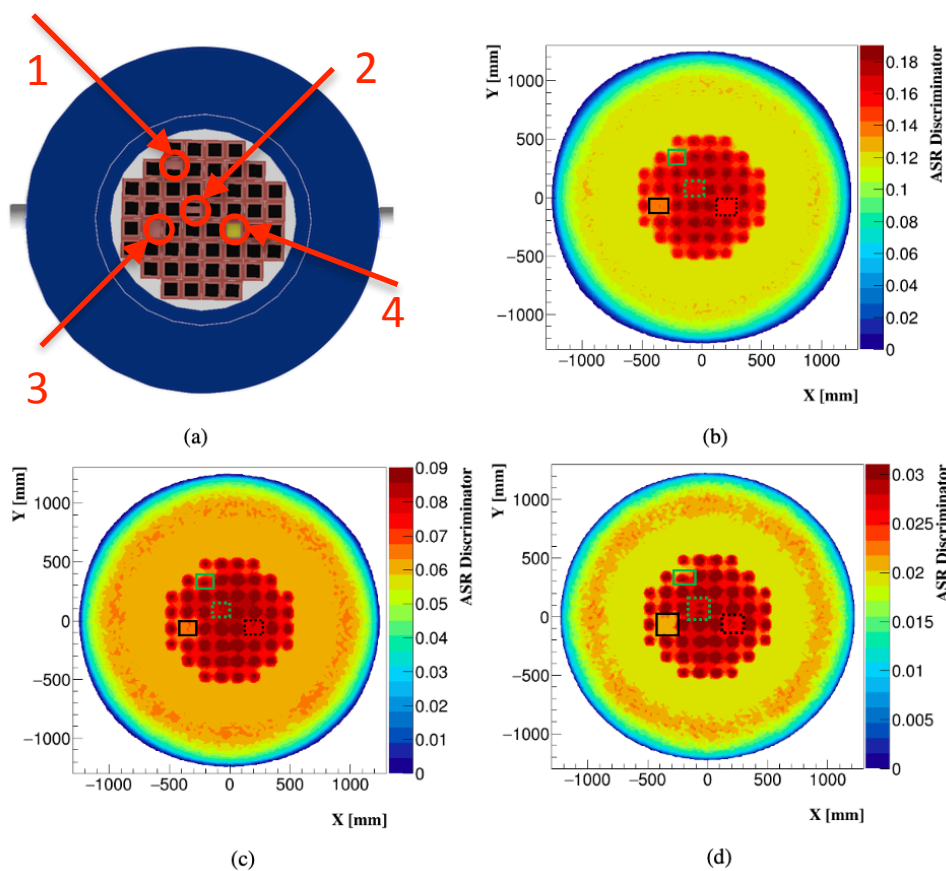


Figure 7: (a) top-view of the V/52 CASTOR showing four baskets which contain an irregularity in their contents (red circles). Comparison of the feature resolutions of the cask’s contents produced by the ASR algorithm when considering (b) 75%, (c) 50% and (d) 25% of the ASR discriminator in each voxel, respectively. The solid and dashed green boxes indicate the half-loaded baskets, while the solid and dashed black boxes indicate the baskets that contain no pellets and copper pellets, respectively. The exposure time was 30 days equivalent.

The results depicted in Figure 7 are for the ASR algorithm which was show to be the best performing the of the 3 algorithms considered for this body of work. The ASR algorithm succeeds in minimising the smearing noise that results from the PoCA assumption. Additional quantiles of 25% and 50% of the ASR discriminator distributions in each voxel are also considered (see Figure 7 (c) and (d)). Comparing the empty basket with the eight surrounding fully loaded baskets produces a CNR value of 2.8 ± 0.25 when 75% of the

discriminator distributions were taken in each voxel. However, considering the 25% quantile of each voxel distribution improves the CNR value about to 5.0 ± 0.3 . Further studies were also performed that considered the feature resolution as a function of muon exposure time. It was found that after 4 days of muon exposure time, the density maps are constrained by the detector's angular resolution and the fuel assemblies inside the image are smeared by the neighbouring baskets.

Section 5: Summary

As documented elsewhere in the WP4 deliverables (D4.1 report), a number of unforeseen challenges, including COVID-19, BREXIT, Freon ban and equipment failures have led to an unfortunately paucity in the amount of empirical data that we have from the muon scattering imaging detector system. However, the simulations performed and reported on above have all been tuned to accurately mimic the configuration and expected performance of the system. With more experimental data, we are confident that the capabilities demonstrated here in our simulations studies, in terms of materials identification, void location, material location and material differentiation would be reflected in our empirical findings.

References

- [1] CHANCE: Characterisation of conditioned radioactive waste, <https://www.chance-h2020.eu/>.
- [2] S. Riggi et al., A Muon tomography imaging algorithms for nuclear threat detection inside large volume containers with the Muon Portal detector, Nuclear instruments & methods in physics research. Section A, Accelerators, spectrometers, detectors and associated equipment 728 (2013) 59–68.
- [3] M. Stapleton, J. Burns, S. Quillin and C. Steer, Angle Statistics Reconstruction: a robust reconstruction algorithm for Muon Scattering Tomography, Journal of instrumentation 9(11) (2014) P11019.
- [4] C.Thomay et al., A binned clustering algorithm to detect high-Z material using cosmic muons, Journal of instrumentation 8(10) (2013) P10013.
- [5] P. Stowell et al., Figures of Merit for the Application of Muon Tomography to the Characterization of Nuclear Waste Drums, WM2019 Conference, March 2019, https://www.researchgate.net/publication/331960072_Figures_Of_Merit_for_the_Application_of_Muon_Tomography_to_the_Characterization_of_Nuclear_Waste_Drums
- [6] S. Agostinelli et al., Geant 4 — a simulation toolkit, Nuclear instruments & methods in physics research. Section A, Accelerators, spectrometers, detectors and associated equipment 506(3) (2003) 250–303.
- [7] Haggmann, D. Lange and D. Wright, Cosmic-Ray Shower Generator (CRY) for Monte Carlo Transport Codes, 2007 IEEE Nuclear Science Symposium Conference Record 2 (2007) 1143–1146.
- [8] M. Mhaidra et al., A robust method to find gas bubbles inside large nuclear waste containers using Muon Tomography, WM2021 Conference, March 2021, https://www.researchgate.net/profile/Mohammed-Mhaidra/publication/350174721_A_robust_method_to_find_gas_bubbles_inside_large_nuclear_waste_container



s_using_Muon_Tomography/links/60545f57299bf1736752b084/A-robust-method-to-find-gas-bubbles-inside-large-nuclear-waste-containers-using-Muon-Tomography.pdf

[9] A quantitative assessment of Imaging High-Z and Medium-Z materials using Muon Scattering Tomography, A.F. Alrheli, et al., submitted to JINST.